# Low frequency oscillations in a plasma with spatially variable field-aligned flow

G. Ganguli, S. Slinker, V. Gavrishchaka, and W. Scales

Citation: Physics of Plasmas (1994-present) **9**, 2321 (2002); doi: 10.1063/1.1445181
View online: http://dx.doi.org/10.1063/1.1445181
View Table of Contents: http://scitation.aip.org/content/aip/journal/pop/9/5?ver=pdfcov
Published by the AIP Publishing

# Low frequency oscillations in a plasma with spatially variable field-aligned flow[a)]

G. Ganguli[b)] and S. Slinker
*Plasma Physics Division, Naval Research Laboratory, Washington, D.C. 20375*

V. Gavrishchaka
*Science Applications International Corporation, McLean, Virginia 22102*

W. Scales
*Bradley Department of Electrical and Computer Engineering, Virginia Polytechnic Institute and State University, Blacksburg, Virginia 24060*

(Received 30 October 2001; accepted 9 November 2001)

The effects of a transverse gradient in the plasma flow velocity parallel to the ambient magnetic field are analyzed. A transverse velocity gradient in the parallel ion flow, even in small magnitude, can increase the parallel phase speed of the ion-acoustic waves sufficiently to reduce ion Landau damping. This results in a significantly lower threshold current for the current driven ion acoustic instability. Ion flow gradients can also give rise to a new class of ion cyclotron waves via inverse cyclotron damping. A broadband wave spectrum with multiple cyclotron harmonics is possible. A combination of the multiple cyclotron harmonic waves can result in spiky electric field structures with their peaks separated by an ion cyclotron period. A spatial gradient in the parallel electron flow is also considered but it is found to play a minimal role in the low frequency regime. Relevance of these to natural plasma environments is discussed. © *2002 American Institute of Physics.*
[DOI: 10.1063/1.1445181]

## I. INTRODUCTION

The classic work of Kindel and Kennel[1] has strongly influenced the interpretation and analysis of space plasma wave observations for decades. Two most enduring notions from this work that are firmly embedded in the space plasma community are that (1) the current driven ion-cyclotron instability (CDICI) has the lowest threshold in the ionospheric plasma environment and therefore it is the likely source for plasma oscillations observed in the ionosphere, and (2) the threshold current necessary for exciting the ion-acoustic instability is orders of magnitude above that of the CDICI. Hence, it is nearly impossible to excite the ion-acoustic waves in the ionosphere for typical magnitudes of observed current, since the ion to electron temperature ratio is of order unity in this region. These have been repeatedly invoked in connection to space plasma observations. However, with the advent of modern high-resolution space probes more detailed observations were possible and it became evident that additional physics, not included in the Kindel and Kennel theory,[1] was necessary to accurately describe the physical underpinnings. Kintner[2] summarized the major discrepancies between the observations and the Kindel and Kennel theory. Some of these are (i) although levels of field-aligned current which are observed are generally subcritical, waves associated with current are nevertheless observed. (ii) While the wave spectrum is expected to be narrowband and structured around cyclotron harmonics, a broadband smooth frequency spectrum is often reported. (iii) While gyroresonant ion heating due to CDICI is possible, rising ion temperature should be self-limiting.[3] However, ion energization is frequently observed associated with broadband waves.[4–8] In addition, although the theory indicates that the threshold for the ion-acoustic instability is much higher than the ion cyclotron instability, ion-acoustic-like waves are observed in the ionosphere.[9–11] More recent observations[12] indicate the existence of discrete wave spectrum at multiples of hydrogen cyclotron harmonics, which would require much higher levels of current.

An obvious physical feature that was left out of the Kindel and Kennel model is transverse localized electric fields such as those observed in the S3-3 satellite data[13,14] and in a number of subsequent space probes. To understand the role of such inhomogeneous transverse electric field, a general kinetic formalism was developed[15–18] and a uniform field-aligned current was subsequently added to this model.[19] Detailed space applications[20,21] highlighted the important role of dc electric fields, especially in broadening the wave spectrum, washing out the cyclotron structures, and ion energization. The theoretical studies inspired a number of laboratory experiments[22–27] specifically designed to test and characterize the physical underpinnings without the space–time ambiguity that is unavoidable in observations made from a moving platform. These laboratory experiments were valuable in understanding the dynamics at smaller scales, which are hardest to detect and characterize in the natural environment because of the statistical nature of *in situ* data collection and limitations arising from space–time ambiguities. A statistical comparison of the theory and laboratory experiments with observations was recently discussed by Hamrin *et al.*[28]

[a)]Paper CI2 2, Bull. Am. Phys. Soc. **46**, 52 (2001).
[b)]Invited speaker.

 

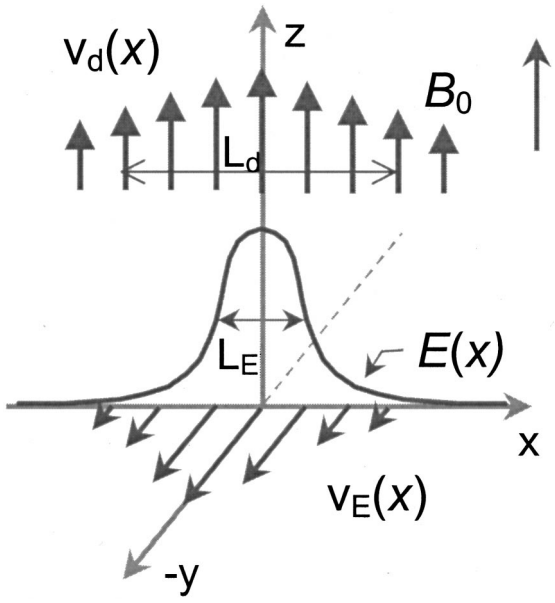


FIG. 1. A sketch of the equilibrium condition.

Although, the inclusion of the transverse dc electric field in the theory was successful in explaining a number of observational features, others such as simultaneous existence of multiple hydrogen cyclotron harmonics,[12] development of parallel coherent electric field sytructures[12] and existence of ion-acoustic wave signature[9–11] remains to be fully understood. Interestingly, these features are generally correlated with localized ion flows parallel to the magnetic field. Hence, we need to understand the role of a transverse gradient in the field-aligned flows in more detail.

## II. THEORY

We[17,29] developed a general nonlocal kinetic formalism for investigation of effects of inhomogeneous parallel and perpendicular flows in the auroral ionosphere. A uniform magnetic field is assumed in the $z$ direction and a nonuniform electric field is assumed in the $x$ direction. Besides a nonuniform $E\times B$ drift $[V_E(x)=-cE(x)/B]$ in the $y$ direction a nonuniform flow along the magnetic field $[V_d(x)]$ is also considered. The plasma density can also be nonuniform in the $x$ direction. The background plasma condition is sketched in Fig. 1. The details of the mathematical derivations can be found in Refs. 17 and 29 and are not repeated here. The effects of a gradient in transverse flows and their space and laboratory applications are summarized in Ref. 18 and references therein. The primary focus of this paper is to highlight the role of a transverse gradient in the parallel flows. In order to do so we will consider the equilibrium transverse electric field scale size to be much larger than the parallel flow scale size (i.e., $L_E \gg L_d$), so that the electric field can be considered to be effectively uniform. The more general case in which inhomogeneity in both parallel and transverse flows is simultaneously operative will be addressed subsequently.

To simplify further, consider a locally linear flow [i.e., $V_{d\alpha}(x)=V_{d\alpha}+(dV_{d\alpha}/dx)x$, where $V_{d\alpha}$ and $(dV_{d\alpha}/dx)$ are constants and $\alpha$ represents the species], and no equilibrium electric field. Also, for simplicity, let $dV_{di}/dx=dV_{de}/dx \equiv dV_d/dx$. Transform to the ion frame (i.e., $V_{di}=0$) so that $V_{de}$ represents the relative electron–ion parallel drift. In the local limit[30,31] these simplify the general dispersion relation to

$$1+\sum_n \Gamma_n(b)F_{ni}+\tau(1+F_{0e})=0,$$

$$F_{ni}=\left(\frac{\omega}{\sqrt{2}|k_z|v_{ti}}\right)Z\left(\frac{\omega-n\Omega_i}{\sqrt{2}|k_z|v_{ti}}\right) - \frac{k_y}{k_z}\frac{dV_d/dx}{\Omega_i}\left[1+\left(\frac{\omega-n\Omega_i}{\sqrt{2}|k_z|v_{ti}}\right)Z\left(\frac{\omega-n\Omega_i}{\sqrt{2}|k_z|v_{ti}}\right)\right], \tag{1}$$

$$F_{0e}=\left(\frac{\omega-k_zV_{de}}{\sqrt{2}|k_z|v_{te}}\right)Z\left(\frac{\omega-k_zV_{de}}{\sqrt{2}|k_z|v_{te}}\right) + \frac{k_y}{k_z}\frac{dV_d/dx}{\mu\Omega_i}\left[1+\left(\frac{\omega-k_zV_{de}}{\sqrt{2}|k_z|v_{te}}\right)Z\left(\frac{\omega-k_zV_{de}}{\sqrt{2}|k_z|v_{te}}\right)\right].$$

Here, $\Gamma_n(b)=I_n(b)\exp(-b)$ where $I_n$ are the modified Bessel function, $b=(k_y\rho_i)^2$, $\rho_i=v_{ti}/\Omega_i$ is the ion gyroradius, $v_{ti,e}$ is the ion (electron) thermal velocity, $\tau=T_i/T_e$, and $\mu=M_i/m_e$ is the ion/electron mass ratio. For no shear (i.e., $dV_d/dx=0$), the dispersion relation reduces to the case for a homogeneous flow.[1,32]

### A. Shear modified ion-acoustic waves

We first discuss low (subcyclotron) frequency ion-acoustic waves[30,31] by keeping only the $n=0$ term for the ions and considering long wavelength $[\Gamma_0(b)\sim 1]$ in Eq. (1) to obtain

$$\sigma^2+\tau\hat{\sigma}^2+\sigma^2\zeta_0Z(\zeta_0)+\tau\hat{\sigma}^2\zeta_eZ(\zeta_e)=0, \tag{2}$$

where

$$\zeta_0=\left(\frac{\omega}{\sqrt{2}|k_z|v_{ti}}\right),\quad \zeta_e=\left(\frac{\omega-k_zV_{de}}{\sqrt{2}|k_z|v_{te}}\right),$$

$$\sigma^2=1-k_yV_d'/k_z\Omega_i,\quad V_d'=dV_d/dx,$$

$$\hat{\sigma}^2=1+k_yV_d'/k_z\Omega_i\mu.$$

Assuming the ions to be fluid ($\zeta_0\gg 1$) and electrons to be Boltzmann ($\zeta_e\ll 1$) and equating the real part of Eq. (2) to zero we get

$$\omega=k_zc_s\sigma/\hat{\sigma}\sim k_zc_s\sigma, \tag{3}$$

where $c_s=(T_e/m_i)^{1/2}$ and $\hat{\sigma}^2\sim 1$ is used since $\mu\gg 1$. For no shear ($dV_{di}/dx=0$, i.e., $\sigma^2=1$) the classical ion-acoustic limit is recovered. If $\sigma^2<0$, then we recover the narrowband D'Angelo instability[33] around $\omega_r=0$ in the drifting ion frame, which has been the subject of numerous space and laboratory applications for over three decades.[34–36]

Surprisingly, except for the classical case ($\sigma^2=1$), the $\sigma^2>0$ regime had not been previously addressed. In this regime Eq. (3) indicates that it is possible to obtain a shear

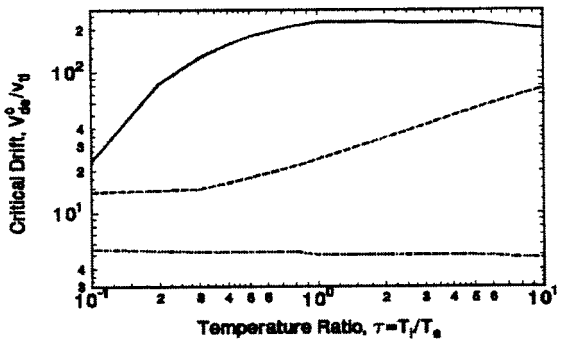


FIG. 2. Temperature ratio dependence of the critical electron drift for the homogeneous ion acoustic and ion cyclotron modes (solid and dashed lines, respectively) and shear modified ion-acoustic waves (dashed–dotted line). Critical drift is minimized over parallel and perpendicular wave numbers. Here $|dV_d/dx|/\Omega_i=0.1$, $\mu=29\,392$ ($o+$plasma), and $\Omega_e/\omega_{pe}=10$.

modified ion-acoustic (SMIA) wave. More interestingly, Eq. (3) also indicates that shear can increase the parallel phase speed ($\omega_r/k_z$) of the ion-acoustic mode by a factor $\sigma$. For a sufficiently large $\sigma$, the phase speed can be increased to reduce ion Landau damping. Consequently, a much lower threshold for the ion-acoustic mode can be realized even for $T_i \geqslant T_e$. The growth rate for the SMIA instability is given by[31]

$$\left(\frac{\gamma}{|k_z|v_{ti}}\right)=\sqrt{\frac{\pi}{8}}\frac{\sigma^2}{\tau^2}\left[\frac{\tau^{3/2}}{\mu^{1/2}}\left(\frac{V_d}{\sigma c_s}-1\right)-\sigma^2\exp(-\sigma^2/2\tau)\right]. \tag{4}$$

The classical ion-acoustic wave growth rate is recovered for $\sigma=1$. Increasing $\sigma$ rapidly lowers the ion Landau damping as seen from the exponential dependence of the second term in the brackets. The critical drift is obtained from Eq. (4) by setting the growth rate to zero and minimizing over the propagation angle ($k_z/k_y$) as is plotted in Fig. 2 (reproduced from Gavrishchaka *et al.*[30]). Here $dV_d/dx=0.1\Omega_i$. It is found that even a small shear can reduce the critical drift for the ion-acoustic instability by orders of magnitude and place it below that of the classical ion cyclotron waves[32] for a wide range of $\tau$ but the waves propagate more obliquely (i.e., small $k_z/k_y$) than their classical counterpart. This is a sharp departure from the conclusion of Kindel and Kennel.[1]

For $k_y/k_z \gg 1$ the magnitude of shear, i.e., $dV_{di}/dx$, necessary for the SMIA waves is very small. This may provide a credible explanation for the observation of ion-acoustic-like waves in ionospheric plasma[9–11] where $T_i \sim T_e$. This may also resolve an important and outstanding debate on the origin of ion-acoustic waves in the solar wind plasmas[37–40] as well as be relevant to the problem of dissipation in a collisionless shock.[41,42] These interesting possibilities have recently inspired a laboratory experiment[43] in the University of Iowa which demonstrated the spontaneous generation of ion-acoustic waves by sheared ion flow along the magnetic field in a Q-machine plasma in which $T_i \sim T_e$. While the SMIA waves can explain the low frequency portion of the spectrum it alone is not sufficient to explain the considerable breadth of the spectrum generally observed in space,[12] which extends from below the oxygen cyclotron frequency to a few hydrogen cyclotron frequencies. This motivates us to extend the idea to higher (cyclotron) frequencies and examine the effects of velocity shear on these frequencies.

### B. Shear driven multiharmonic ion cyclotron waves

To study the ion cyclotron frequency regime we return to Eq. (1) but relax the constraints of low frequency and long wavelength used in Sec. II A. We first examine how a gradient in the parallel plasma flow affects the threshold condition for ion cyclotron waves by analyzing the expression for critical relative drift for the ion cyclotron waves in small and large shear limits. For the marginal stability condition ($\gamma=0$) the imaginary part of the dispersion relation, Eq. (1), is set equal to zero,

$$\sum_n \Gamma_n\left[\left(\zeta_0-\frac{k_yV_d'}{k_z\Omega_i}\zeta_n\right)\mathrm{Im}\,Z(\zeta_n)\right] + \tau\left(1+\frac{k_yV_d'}{k_z\Omega_i\mu}\right)\zeta_e\,\mathrm{Im}\,Z(\zeta_e)=0, \tag{5}$$

where

$$\zeta_n=\left(\frac{\omega-n\Omega_i}{\sqrt{2}|k_z|v_{ti}}\right).$$

Dividing Eq. (5) throughout by $\zeta_0$ and considering $\zeta_e \ll 1$, we get

$$\sum_n \Gamma_n\left[\left(1-\frac{k_yV_d'}{k_z\Omega_i}\left(1-\frac{n\Omega_i}{\omega_r}\right)\right)\exp\left\{-\left(\frac{\omega_r-n\Omega_i}{\sqrt{2}|k_z|v_{ti}}\right)^2\right\}\right] + \frac{\tau^{3/2}}{\mu^{1/2}}\left(1+\frac{k_yV_d'}{k_z\Omega_i\mu}\right)\left(\frac{\omega_r-k_zV_{dc}}{\omega_r}\right)=0. \tag{6}$$

Under ordinary conditions $(k_y/k_z)(dV_d/dx)/\Omega_i \ll \mu$, which implies that the shear in the electron flow is not as critical as it is in the ion flow and can be ignored. Since only the resonant harmonic term dominates, Eq. (6) can be simplified to obtain an expression for the critical relative drift,

$$V_{dc}=\frac{\omega_r}{k_z}\left[1+\Gamma_n(b)\frac{\mu^{1/2}}{\tau^{3/2}}\left\{1-\frac{k_yV_d'}{k_z\Omega_i}\left(1-\frac{n\Omega_i}{\omega_r}\right)\right\}\times\exp\left(-\frac{(\omega_r-n\Omega_i)^2}{2k_z^2v_{ti}^2}\right)\right]. \tag{7}$$

For no shear, $dV_d/dx=0$, the critical drift reduces to

$$V_{dc}^0=\frac{\omega_r}{k_z}\left[1+\Gamma_n(b)\frac{\mu^{1/2}}{\tau^{3/2}}\exp\left(-\frac{(\omega_r-n\Omega_i)^2}{2k_z^2v_{ti}^2}\right)\right]. \tag{8}$$

This is the critical drift for the homogeneous current driven ion cyclotron instability.[32,1] Since the relative sign between the two terms within the brackets is positive and each term is positive definite, the critical drift is always greater than the wave phase speed and increases for higher harmonics since $\omega_r \sim n\Omega_i$.

From Eq. (7) it may appear that for small but nonnegligible and positive values of $(k_y/k_z)(1-n\Omega_i/\omega_r)\times(dV_d/dx)/\Omega_i$ there can be a substantial reduction in the critical drift for the current driven ion cyclotron instability[32]

because of reduction in the ion cyclotron damping. However, this is not possible and can be understood by rewriting Eq. (7) as

$$\frac{V_{dc}}{V_{dc}^0}=1-\left\{1-\frac{(\omega_r/k_z)}{V_{dc}^0}\right\}\left(\frac{k_yV_d'}{k_z\Omega_i}\right)\left(1-\frac{n\Omega_i}{\omega_r}\right), \tag{9}$$

where the second term represents the correction to the critical drift for the current driven ion cyclotron instability due to shear. A necessary condition for the CDICI is that $V_d>\omega_r/k_z$. For a given magnitude of $|dV_d/dx|/\Omega_i\ll 1$, it is clear from Eq. (9) that the shear correction is small unless the ratio $k_y/k_z$ can be made large. However, as $k_y$ increases, the real frequency of the wave approaches harmonics of the ion cyclotron frequency and consequently $(1-n\Omega_i/\omega_r)$ becomes very small which makes the shear correction small. Alternately, when $k_z$ decreases the wave phase speed increases and the condition $V_d>\omega_r/k_z$ is violated. Thus, for realistic (small to moderate) values of the shear magnitude, the reduction in the threshold current for the current driven ion cyclotron instability by a gradient in the ion parallel flow is minimal at best. This is unlike the current driven ion-acoustic mode case as discussed in Sec. II A.

Although shear is ineffective in reducing the threshold current for the ion cyclotron instability, it allows for a novel method to extract free energy from the spatial gradient of the ion flow, which does not involve a resonance of parallel phase speed with the relative drift speed. To illustrate this we return to Eq. (7) and consider the limit $(1-n\Omega_i/\omega_r)\times(k_y/k_z)(dV_d/dx)/\Omega_i\gg 1$, in which Eq. (7) reduces to

$$V_{dc}=\frac{\omega_r}{k_z}\left[1-\Gamma_n(b)\left(1-\frac{n\Omega_i}{\omega_r}\right)\frac{\mu^{1/2}}{\tau^{3/2}}\left(\frac{k_y}{k_z}\frac{dV_d/dx}{\Omega_i}\right)\times\left\{\exp\left(-\frac{(\omega_r-n\Omega_i)^2}{2k_z^2v_{ti}^2}\right)\right\}\right]. \tag{10}$$

Each term of Eq. (10) is still positive definite but the relative sign between them is now negative, which allows for $V_{dc}=0$. In this regime, the ion flow gradient can support ion cyclotron waves. The physical process can be understood by examining the expression for the growth rate for these waves, which can be expressed as

$$\frac{\gamma}{\Omega_i}=\sqrt{\frac{\pi}{2}}\left(\frac{\Omega_i}{|k_z|v_{ti}}\right)\frac{\left[\frac{\tau^{3/2}}{\mu^{1/2}}\left(\frac{V_{de}}{(\omega_r/k_z)}-1\right)-\sum_n\Gamma_n\left\{1-\frac{k_yV_d'}{k_z\Omega_i}\left(1-\frac{n\Omega_i}{\omega_r}\right)\right\}\exp\left(-\frac{(\omega_r-n\Omega_i)^2}{2k_z^2v_{ti}^2}\right)\right]}{\sum_{n>0}\frac{4n^2\Gamma_n}{(\omega^2/\Omega^2-n^2)^2}}. \tag{11}$$

From (11) we see that

$$\frac{\gamma}{\Omega_i}\propto\left[\frac{\tau^{3/2}}{\mu^{1/2}}\left(\frac{V_{de}}{(\omega_r/k_z)}-1\right)-\sum_n\Gamma_n\left\{1-\frac{k_yV_d'}{k_z\Omega_i}\left(1-\frac{n\Omega_i}{\omega_r}\right)\right\}\exp\left(-\frac{(\omega_r-n\Omega_i)^2}{2k_z^2v_{ti}^2}\right)\right]. \tag{12}$$

The first term in the brackets represents a balance between growth due to the field-aligned drift and electron Landau damping while the second term represents cyclotron damping. Provided the drift speed exceeds the wave phase speed and the magnitude of the first term is large enough to overcome the cyclotron damping a net growth for the ion cyclotron waves can be realized. This is the classical case where inverse electron Landau damping leads to wave growth.[32] For the homogeneous case (i.e., $dV_d/dx=0$), the second term is positive definite and always leads to damping. However, if $(1-n\Omega_i/\omega_r)\ (k_y/k_z)(dV_d/dx)/\Omega_i>1$ then the sign of the cyclotron damping can be changed and the second term can provide a net growth even for $V_{de}=0$. This new possibility for wave growth is facilitated by velocity shear via inverse cyclotron damping and favors short perpendicular and long parallel wavelengths which makes the term proportional to shear large even when the magnitude of shear is small. A necessary condition for ion cyclotron instability due to inverse cyclotron damping is

$$\left(1-\frac{n\Omega_i}{\omega_r}\right)\left(\frac{k_y}{k_z}\frac{dV_d/dx}{\Omega_i}\right)=\left(1-\frac{n\Omega_i}{\omega_r}\right)\left(\frac{V_{py}}{V_{pz}}\frac{dV_d/dx}{\Omega_i}\right)>1, \tag{13}$$

where $V_{py}$ and $V_{pz}$ are phase velocities in the $y$ and $z$ directions.

Another noteworthy feature introduced by the ion flow gradient is in the generation of higher cyclotron harmonics. From Eq. (8) we see that in the homogeneous case the $n$th harmonic requires a much larger drift than the first harmonic. However, for $\omega_r\sim n\Omega_i$ the critical shear necessary to excite the $n$th harmonic of the gradient-driven ion cyclotron mode, can be expressed as

$$\frac{(dV_d/dx)_c}{\Omega_i}\sim\frac{\tau^{3/2}}{\mu^{1/2}}\left(\frac{k_z}{k_y}\right)\left(\frac{1+\tau-\Gamma_0(b)}{\Gamma_n^2(b)}\right). \tag{14}$$

For short wavelengths, i.e., $b\gg 1$, $\Gamma_n\sim 1/\sqrt{2\pi b}$ and hence, to leading order the critical shear is independent of the harmonic number. Consequently, a number of higher harmonics can be simultaneously generated by the shear magnitude necessary for exciting the fundamental harmonic. This is quantitatively shown in Fig. 2 of Ref. 44, which shows about 20 ion cyclotron harmonics can be generated for typi-

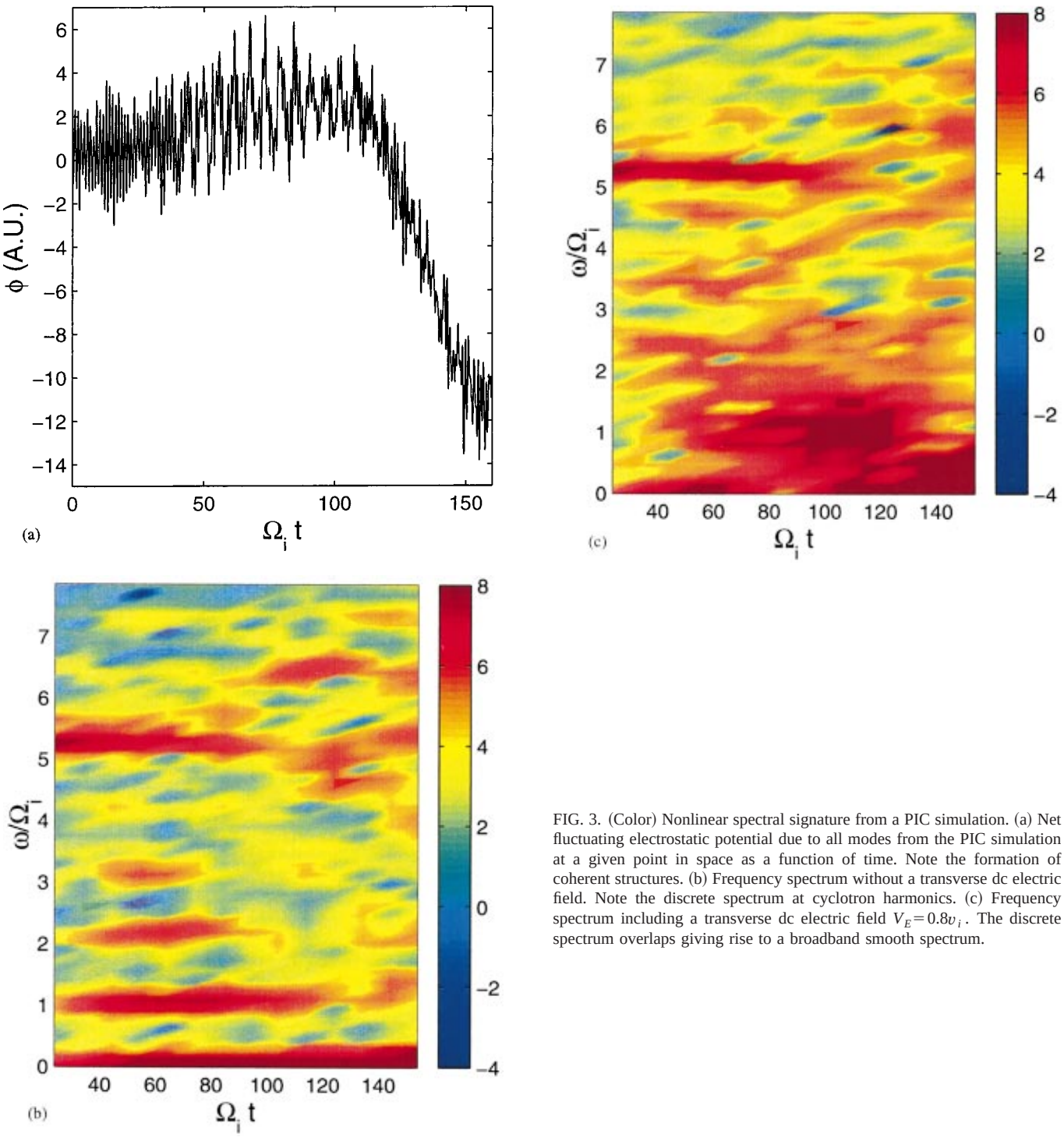


FIG. 3. (Color) Nonlinear spectral signature from a PIC simulation. (a) Net fluctuating electrostatic potential due to all modes from the PIC simulation at a given point in space as a function of time. Note the formation of coherent structures. (b) Frequency spectrum without a transverse dc electric field. Note the discrete spectrum at cyclotron harmonics. (c) Frequency spectrum including a transverse dc electric field $V_E = 0.8 v_i$. The discrete spectrum overlaps giving rise to a broadband smooth spectrum.

cal ionospheric plasma parameters. This figure also shows that when the Doppler broadening due to transverse dc electric fields that are frequently observed in the ionosphere is also taken into account, the discrete spectra around individual cyclotron harmonics overlap to form a continuous broadband spectrum such as those found in satellite observations. Effects[20,21] of transverse electric field alone could not produce such a large spectral bandwidth. This remarkable ability of ion velocity shear to excite multiples of ion cyclotron harmonics simultaneously via inverse cyclotron damping is similar to the ion cyclotron maser mechanism.[45] However, important differences with the ion cyclotron maser instability exist. The ion cyclotron maser instability is an electromagnetic nonresonant instability while we discuss the electrostatic limit of a resonant instability. Electromagnetic generalization of our mechanism is possible and will be addressed in the future. Also, in our mechanism the background magnetic field is uniform unlike the ion cyclotron maser mechanism. An additional important feature that can be gleaned from Eq. (14) is that for $k_z \to 0$, $(dV_d/dx)_c \to 0$. This is borne out from the numerical solution of the unapproximated dispersion relation, Eq. (1).

### C. Nonlinear signatures

We have examined the nonlinear signatures of the ion cyclotron oscillations by a standard 2D 3 V electrostatic particle-in-cell (PIC) simulation model[44] including full ion dynamics and gyrocenter approximation for the electrons.[46] To clearly resolve short wavelength modes we used 900 particles per cell with grid size $\Delta=\lambda_D=0.2\rho_i$ and used $\mu=1837$. A drifting Maxwellian $(H+,e-)$ plasma is initially loaded, with equal ion and electron temperatures. The magnetic field is slightly tilted such that $k_z/k_y=0.01$. A parallel drift velocity $V_d(x)$ is assigned to ions. The magnitude of the flow is initially specified and not reinforced during the simulation. To characterize the role of spatial gradient in the flow, the relative drift between the ions and the electrons, i.e., field aligned current, is kept at a minimum. Its value does not exceed $3v_{ti}$ locally while on average it is negligible. Periodic boundary conditions are used in both $x$ and $y$ directions. The magnitude of shear, $|dV_d/dx|_{\max}=2\Omega_i$ is used for the simulation. For this case $L_x=64\lambda_D$ and $L_y=64\lambda_D$.

In Fig. 2 of Ref. 44 we discussed the linear spectrum with and without the transverse dc electric field. Figure 3 is a comparison of the nonlinear spectral character without and with a uniform transverse dc electric field. Figure 3(a) is the net fluctuating electrostatic potential due to all the excited modes in the simulation at a given point in space. Low and high frequency modes are spontaneously generated. Also note the formation of spiky structures separated by ion-cyclotron times. Figure 3(b) is the wave spectrum without a transverse electric field. Several ion cyclotron harmonics are excited with discrete harmonic structure. In Fig. 3(c) we add a uniform transverse dc electric field with $V_E=0.8vi$. The washing out of the harmonic structure and broadening of the spectrum due to overlap of the discrete spectra around $\omega=0$ and multiple cyclotron harmonics becomes evident.

The simulations [see Fig. 4(c) in Ref. 44] indicate that coherent parallel electric field structures with their peaks separated in time by roughly the ion cyclotron period develop. This is also reflected in the electrostatic potential as shown in Fig. 3(a). Interestingly, similar structures are also seen in spacecraft data[12,47] although it is not clear how these structures originate in space plasmas. As discussed by Temerin *et al.*,[47] these structures could be steepened ion-cyclotron waves. Temerin *et al.* reported observing steepened electrostatic hydrogen cyclotron waves in the auroral zone at altitudes between 5000 and 8000 km. These waves have often been observed simultaneously with magnetic field aligned beams of 0.5 to 16 keV $H^+$ and $O^+$ ions flowing out of the auroral region. The spectrum of these waves contains multiple harmonics of the ion cyclotron frequency, consistent with the observed sawtooth and spiky wave forms. Temerin *et al.*[47] and Chaturvedi[48] have examined one-dimensional nonlinear traveling wave solutions for the Sagdeev potential which describes electrostatic ion cyclotron waves in a fluid plasma. The solutions obtained often have a striking resemblance to the wave forms observed.[47] However, these solutions only imply that a nonlinear state with features similar to the observations is possible. They do not elucidate either the formation mechanism and uniqueness or the ambient ionospheric conditions most conducive to their generation.

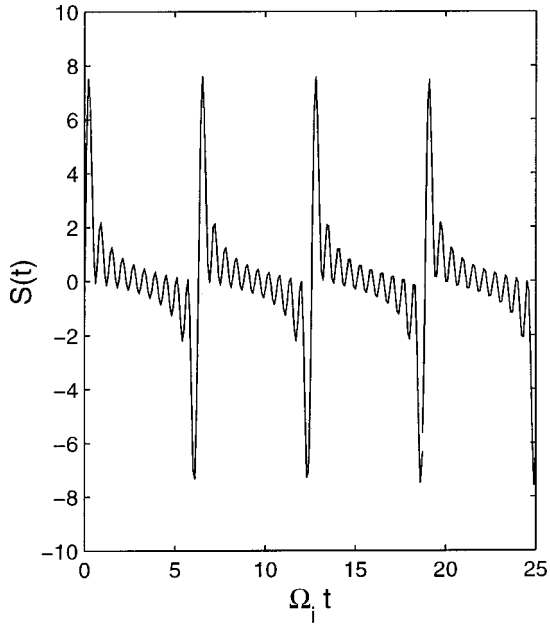


FIG. 4. An illustrative time series $S(t)=\Sigma_n \sin(n\omega t+\delta)$ with $n=10$ and $\delta=0$. As multiple ion cyclotron harmonic waves are generated they can combine to form such structures linearly and then evolve to the nonlinear stage. Note that the peaks of these structures are separated by the ion cyclotron period.

Our analysis along with PIC simulations suggest that these are related to the shear-driven multiple ion cyclotron harmonic waves. Once the multiple harmonic waves are generated they can combine to form the coherent spiky electric field structures with their peaks separated by ion cyclotron time scales. To illustrate this consider a model time series, $S(t)=\Sigma_n \sin(n\omega t+\delta)$, with $\omega\sim\Omega_i$. Figure 4 shows that linear combination leads to spiky structures with peaks separated by ion cyclotron time scales are formed. We have used $n=10$ and $\delta=0$ in this plot. The formation of these structures is essentially a linear phenomenon and morphologically they appear to be very similar to the coherent structures seen in the saturated stage of the simulation. The amplitude of these structures increase with increasing harmonic number.

In the above illustration we maintained the phase $\delta=0$ for all the waves. This is an idealization intended only to emphasize a point. To test the integrity of these linear combinations when waves with a variety of phases are present we introduced a random phase $\delta_n$. There was little difference in the structures when $\delta_n$ was restricted to a small angular spread. This is quite encouraging for the structural integrity of these linear combinations. Even in the most extreme case when $\delta_n$ was uniformly distributed between 0 and $2\pi$, we found that while the details of the structures in between the peaks may alter, the peaks still remain distinct and separated by the ion cyclotron period. Similarly, we have also tested the effects of a random noise, i.e., $S(t)=\Sigma_n \sin(n\omega t+\delta_n)+A$, where $A$ is a uniform random variable between $-3$ and 3 and found that the structures remain more-or-less intact. These imply that the linear combinations are quite robust and can last long enough for the phases to get locked due to nonlinear processes and develop into coherent structures.

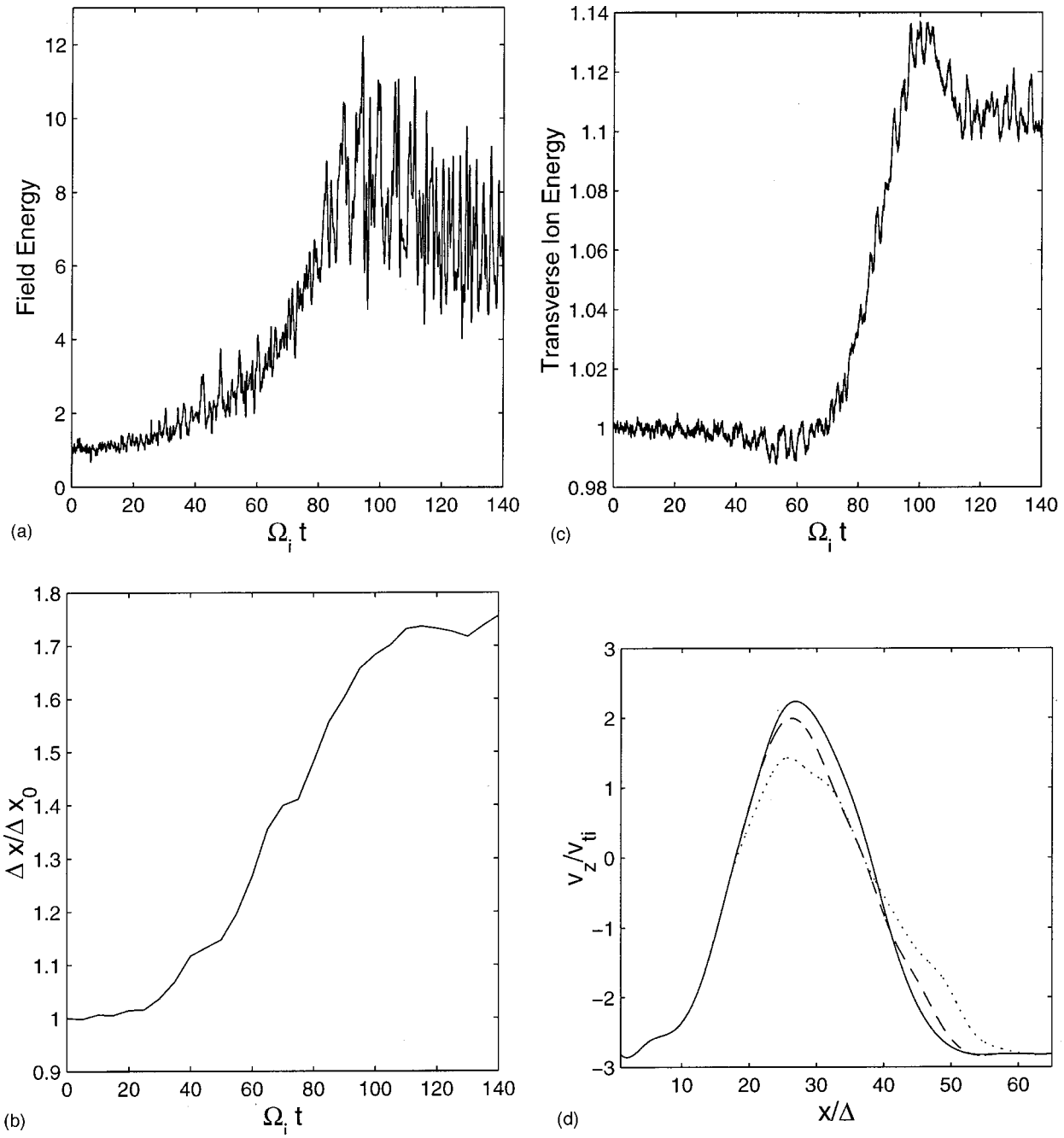


FIG. 5. Mesoscale effects in the PIC simulation due to ion cyclotron waves. (a) Total field energy normalized by its initial value. (b) Particle diffusion characterized by the spatial spread of marked particles normalized by its initial value. (c) Transverse ion energy normalized by its initial value. (d) Relaxation of ion flow profile. Initial profile is reduced in magnitude and gradient. The solid, dashed, and dotted lines correspond to $\Omega_i t = 0$, 60, and 100. Because of the two-dimensional simulation box only one slope is unstable which is consistent with Eq. (13).

Therefore, a linear combination of spontaneously generated multiharmonic ion cyclotron waves due to ion flow gradient could well be the seed that leads to the coherent electric field structures in the nonlinear stage as seen in our simulation [Fig. 4(c) in Ref. 44] and are remarkably similar to those observed in the satellite data.[12,44]

The mesoscale effects of the instability (normalized by their initial values) are given in Fig. 5. To highlight the role of shorter wavelength ion cyclotron waves we remove the longer wavelengths by using a $(64\times16)\lambda_D$ size simulation box in this case. Figure 5 shows the time dependence of the total wave energy [Fig. 5(a)] correlated with diffusion [Fig. 5(b)] and transverse ion energization [Fig. 5(c)]. Broadband waves are usually associated with ion energization in space plasmas.[4–8] The waves are generated in the shear region as required by phase relation Eq. (13) for the 2D system, which imposes a unique sign of $k_z/k_y$. Figure 5(d) illustrates relaxation of the flow gradient due to wave-induced viscosity.

Figure 6 is a plot of electron flux as a function of time in the region of wave activity. We see that as the wave emerges out of the thermal noise and matures, it accelerates the ambient electrons and imprints on them a modulation at the

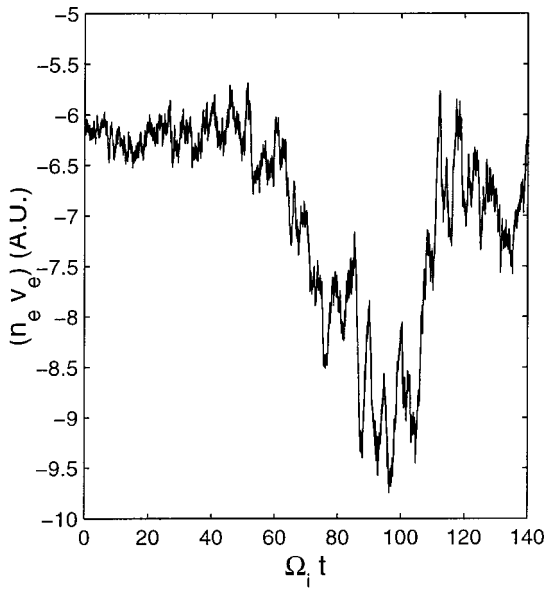


FIG. 6. Self-consistent electron flux as a function of time. Note that as waves mature the electron flux is enhanced due to electron acceleration and modulated at the wave frequency.

wave frequency, in this case near $\omega = 0$ and the ion cyclotron frequency as shown in Fig. 3. This has important implications for the phenomenon of auroral flicker.[49] The observation of narrowband auroral flicker[49] is explained to be a consequence of the wave-particle interaction at high (magnetospheric) altitude between the ambient electrons and electromagnetic ion cyclotron waves found in the magnetosphere although their origin is uncertain. After being energized and modulated in the magnetosphere, the electrons travel all the way down to around 110 kms where their impacts with the neutral molecular oxygen and nitrogen produce dissociation leading to chemical processes that ultimately results in the auroral illumination. In this model the local ionospheric processes do not affect the electrons. Our simulation indicates that the ionospheric processes can affect the electron flux by producing waves locally, which can modulate and energize the electrons. However, for a more definitive conclusion regarding the observation, our model must include a multispecies (oxygen–hydrogen) population and inhomogeneous transverse electric fields, which are features of the plasma background in the ionosphere and can determine the wave frequency. The generalized model may also clarify the cause for the more recent observation[50] of broadband auroral flicker, which is currently not well understood. Our simulations suggest that the broadband waves generated by the combination of inhomogeneous ion parallel flow and a localized transverse dc electric field could be an important factor in the origin of broadband auroral flicker. This possibility will be further explored in the future.

## III. DISCUSSION

We have re-examined the role of spatial variability in the flows along the magnetic field in the interpretation and analysis of observations of auroral plasma phenomena. Since the first paper on this topic by D'Angelo in 1965, numerous space and laboratory applications followed and the field rapidly developed over the last three and one-half decades. However, these developments focused solely on the condition that $\sigma^2 < 0$. Our contribution to this matured field was simply to return to the beginning and ask what if $\sigma^2 > 0$? The primary motivation for this was the persistent observations of ion-acoustic-like turbulence in auroral plasmas[9–11] with nearly equal ion and electron temperatures that could not be easily understood. In Sec. II A we discussed how a modest amount of spatial variability in the ion flow could enable the generation of ion-acoustic waves in a plasma by significantly reducing the ion Landau damping even when the ion temperature exceeds the electron temperature. Subsequently, motivated by auroral plasma observations of broadband low frequency waves and multiple hydrogen cyclotron waves, we extended our model to these higher frequencies. We found that a spatial variability in the ion flow along the magnetic field can also profoundly alter the generation and characteristics of ion cyclotron waves. In Sec. II B we discussed how a new class of ion cyclotron waves can be excited by the shear in the flow via inverse cyclotron damping even for zero relative drift and easily give rise to multiple harmonics of ion cyclotron waves simultaneously for ordinary plasma parameters.

We discussed the nonlinear signatures using a numerical particle-in-cell simulation model. The simulations provided the nonlinear signature of broadband frequency spectrum, which are discretely localized around cyclotron harmonics. When the effect of a transverse dc electric field is also accounted for in the simulation these discrete spectra begin to overlap and form a broadband continuous frequency spectrum. Simultaneous generation of multiple cyclotron harmonics leads to the formation of coherent electric field structures and gives rise to modulation in electron flux self-consistently. In the nonlinear phase we see cross-field transport both in particle position and velocity resulting in relaxation of the initial velocity gradient profile. The wave-particle interaction also leads to ion energization. Since most of these phenomena are intimately linked to the simultaneous generation of multiple cyclotron harmonics, the key ingredient for the success of the model is the role of spatial variability in the ion flow parallel to the magnetic field. This can be more clearly appreciated when we contrast our simulation with those of Ishiguro *et al.*[51] who ignored the ion flow but considered an inhomogeneous electron flow with respect to the ions (similar to the equilibrium we had previously analyzed[52]). The Ishiguro *et al.* simulations[51] do not generate the multiples of ion cyclotron harmonics and consequently miss much of the physics critical to the upward current region of the earth's auroral zone. Since there is no ion velocity gradient in their model, they cannot access the inverse cyclotron damping regime and exploit the benefits offered by the ion velocity gradient such as reduction of the threshold current and simultaneous generation of multicyclotron harmonic waves, etc. Clearly, as far as auroral plasma dynamics in the low frequency regime is concerned, it appears that a spatial variability in the ion flow is more important than it is in the electron flow and should not be neglected.

For further accuracy in reproducing the auroral phenom-

ena we need to incorporate additional physics currently not included in the model. At higher altitudes (~4000 K ms) the plasma is characterized by temperature anisotropy.[53] Currently, we are addressing this.[54] Since the ionospheric altitudes of interest to us contain both oxygen and hydrogen plasmas, we have to consider the multispecies effects. The model is presently electrostatic while observations also indicate magnetic fluctuations. The model will have to be generalized to include electromagnetic effects. However, our experience with electromagnetic effects associated with transverse flow[55,56] indicates that while the modes have magnetic signatures associated with them, the electrostatic model can explain the bulk of the physics at smaller scales. We also note that recent statistical study of solar plasmas indicate the existence of multiple harmonics of electromagnetic ion cyclotron waves in the solar plasma environment.[57] Possible application of our model to the solar plasma environment will be considered in the future.

## ACKNOWLEDGMENTS

Numerous stimulating discussions with R. Merlino, N. D'Angelo, D. Knudsen, C. Chaston, J. McFadden, R. Ergun, and C. Carlson are acknowledged.

This work is supported by the Office of Naval Research and the National Aeronautics and Space Administration.

[1] J. M. Kindel and C. F. Kennel, J. Geophys. Res. **76**, 3055 (1971).
[2] P. M. Kintner, Phys. Fluids B **4**, 2264 (1992).
[3] P. J. Palmadesso, T. P. Coffey, S. L. Ossakow, and K. Papadopolous, Geophys. Res. Lett. **1**, 105 (1974).
[4] R. E. Erlandson, L. J. Zanetti, M. H. Acuna, A. I. Eriksson, L. Eliasson, M. H. Boehm, and L. G. Blomberg, Geophys. Res. Lett. **21**, 1855 (1994).
[5] E. J. Lund, E. Mobius, L. Tang, L. M. Kistler, M. A. Popecki, D. M. Klumpar, W. K. Peterson, E. G. Shelley, B. Klecker, D. Hovestadt, M. Temerin, R. E. Ergun, J. P. McFadden, C. W. Carlson, F. S. Mozer, R. C. Elphic, R. J. Strangeway, C. A. Cattell, and R. F. Pfaff, Geophys. Res. Lett. **25**, 2049 (1998).
[6] D. J. Knudsen, J. H. Clemmons, and J.-E. Wahlund, J. Geophys. Res. **103**, 4171 (1998).
[7] K. A. Lynch, R. L. Arnoldy, P. M. Kinter, and J. Bonnell, Geophys. Res. Lett. **23**, 3293 (1996).
[8] P. Norqvist, M. Andre, and M. Tyrland, J. Geophys. Res. **103**, 23459 (1998).
[9] D. J. Knudsen and J. E. Wahlund, J. Geophys. Res. **103**, 4157 (1998).
[10] J.-E. Wahlund, P. Louran, T. Chust, H. de Feraudy, R. Roux, B. Holback, B. Cabrit, A. I. Ericksson, P. M. Kintner, M. C. Kelley, J. Bonnell, and C. Chesney, Geophys. Res. Lett. **21**, 1835 (1994).
[11] J.-E. Wahlund, A. I. Eriksson, B. Holback, M. H. Boehm, J. Bonnell, P. M. Kintner, C. E. Seyler, J. H. Clemmons, L. Eliasson, D. J. Knudsen, P. Norqvist, and L. J. Zanetti, J. Geophys. Res. **103**, 4343 (1998).
[12] R. E. Ergun, C. W. Carlson, J. P. McFadden, F. S. Mozer, G. T. Delory, W. Peria, C. C. Chaston, M. Temerin, R. Elphic, R. Strangeway, R. Pfaff, C. A. Cattell, D. Klumpar, E. Shelly, W. Peterson, E. Moebius, and L. Kistler, Geophys. Res. Lett. **25**, 2025 (1998).
[13] M. C. Kelley and C. W. Carlson, J. Geophys. Res. **82**, 2343 (1977).
[14] F. S. Mozer, C. W. Carlson, M. K. Hudson, R. B. Torbert, B. Parady, J. Yatteau, and M. C. Kelley, Phys. Rev. Lett. **38**, 292 (1977).
[15] G. Ganguli, Y. C. Lee, and P. Palmadesso, Phys. Fluids **28**, 761 (1985).
[16] G. Ganguli, P. Palmadesso, and Y. C. Lee, Geophys. Res. Lett. **12**, 643 (1985).
[17] G. Ganguli, Y. C. Lee, and P. J. Palmadesso, Phys. Fluids **31**, 823 (1988).
[18] G. Ganguli, Phys. Plasmas **4**, 1544 (1997).
[19] G. Ganguli and P. J. Palmadesso, Geophys. Res. Lett. **15**, 103 (1988).
[20] V. Gavrishchaka, M. Koepke, and G. Ganguli, Phys. Plasmas **3**, 3091 (1996).
[21] V. V. Gavrishchaka, M. E. Koepke, and G. I. Ganguli, J. Geophys. Res. **102**, 11653 (1997).
[22] W. E. Amatucci, M. E. Koepke, J. J. Carroll III, and T. E. Sheridan, Geophys. Res. Lett. **21**, 1595 (1994).
[23] M. E. Koepke, W. E. Amatucci, J. J. Carroll III, and T. E. Sheridan, Phys. Rev. Lett. **72**, 3355 (1994).
[24] W. E. Amatucci, D. N. Walker, J. A. Antoniades, D. Duncan, G. Ganguli, V. Gavrishchaka, J. H. Bowles, and M. E. Koepke, Phys. Rev. Lett. **77**, 1978 (1996).
[25] M. E. Koepke, J. J. Carroll III, M. W. Zintl, C. A. Selcher, and V. Gavrishchaka, Phys. Rev. Lett. **80**, 1441 (1998).
[26] W. E. Amatucci, J. Geophys. Res. **104**, 14481 (1999).
[27] D. N. Walker, W. E. Amatucci, G. Ganguli, J. A. Antoniades, J. H. Bowles, D. Duncan, V. Gavrishchaka, and M. E. Koepke, Geophys. Res. Lett. **24**, 1187 (1997).
[28] M. Hamrin, M. Andre, G. Ganguli, V. Gavrishchaka, M. Koepke, M. Zintle, N. Ivchenko, T. Karlsson, and J. Clemmons, J. Geophys. Res. **106**, 10803 (2001).
[29] G. Ganguli, M. J. Keskinen, R. Romero, R. Heelis, T. Moore, and C. Pollock, J. Geophys. Res. **99**, 8873 (1994); G. Ganguli, *Geophysical Monograph 93* (American Geophysical Union, Washington, DC, 1995), p. 23.
[30] V. Gavrishchaka, S. B. Ganguli, and G. Ganguli, Phys. Rev. Lett. **80**, 728 (1998).
[31] V. Gavrishchaka, S. B. Ganguli, and G. Ganguli, J. Geophys. Res. **104**, 12683 (1999).
[32] W. E. Drummond and M. N. Rosenbluth, Phys. Fluids **5**, 1507 (1962).
[33] N. D'Angelo, Phys. Fluids **8**, 1748 (1965).
[34] P. J. Catto, M. N. Rosenbluth, and C. S. Liu, Phys. Fluids **16**, 1719 (1973).
[35] J. D. Huba, J. Geophys. Res. **86**, 8991 (1981).
[36] S. P. Gary and S. J. Schwartz, J. Geophys. Res. **85**, 2978 (1980).
[37] D. A. Gurnett and R. R. Anderson, J. Geophys. Res. **82**, 632 (1977).
[38] D. A. Gurnett and L. A. Frank, J. Geophys. Res. **83**, 58 (1978).
[39] D. A. Gurnett, E. Marsch, W. Philipp, R. Schwenn, and H. Rosenbauer, J. Geophys. Res. **84**, 2029 (1979).
[40] S. A. Fuselier and D. A. Gurnett, J. Geophys. Res. **89**, 91 (1984).
[41] A. A. Galeev, *Physics of Solar Planetary Environments* (American Geophysical Union, Washington, DC, 1976), Vol. 1, p. 464.
[42] D. Winske, *Geophysical Monograph* 35 (American Geophysical Union, Washington, DC, 1985), p. 225.
[43] E. Agrimson, N. D'Angelo, and R. L. Merlino, Phys. Rev. Lett. **86**, 5282 (2001).
[44] V. V. Gavrishchaka, G. I. Ganguli, W. A. Scales, S. P. Slinker, C. C. Chaston, J. P. McFadden, R. E. Ergun, and C. W. Carlson, Phys. Rev. Lett. **85**, 4285 (2000).
[45] K. T. Tsang and B. Hafizi, Phys. Fluids **30**, 804 (1987).
[46] C. K. Birdsall and A. B. Langdon, *Plasma Physics Via Computer Simulations* (McGraw-Hill, New York, 1985); T. Tajima, *Computational Plasma Physics* (Addison-Wesley, New York, 1988).
[47] M. Temerin, M. Woldorff, and F. S. Mozer, Phys. Rev. Lett. **43**, 1941 (1979).
[48] P. K. Chaturvedi, Phys. Fluids **19**, 1064 (1976).
[49] M. Temerin, J. P. McFadden, M. Boehm, C. W. Carlson, and W. Lotko, J. Geophys. Res. **91**, 5769 (1986).
[50] M. G. McHarg, D. L. Hampton, and H. C. Stenbaek-Nielson, Geophys. Res. Lett. **25**, 2637 (1998).
[51] S. Ishiguro, T. Sato, H. Takamaru, and The Complexity Simulation Group, Phys. Rev. Lett. **78**, 4761 (1997); S. Ishiguro, T. Sato, H. Takamaru, K. Watanabe, and The Complexity Simulation Group, Phys. Plasmas **4**, 2886 (1997); S. Ishiguro, T. Sato, H. Takamaru, and The Complexity Simulation Group, J. Plasma Phys. **61**, 407 (1999).
[52] G. Ganguli, P. Bakshi, and P. Palmadesso, J. Geophys. Res. **89**, 945 (1984); P. Bakshi, G. Ganguli, and P. Palmadesso, Phys. Fluids **26**, 1808 (1983).
[53] C. Cattell, R. Bergmann, K. Sigsbee, C. Carlson, C. Chaston, R. Ergun, J. McFadden, F. S. Mozer, M. Temerin, R. Strangeway, R. Elphic, L. Kistler, E. Moebius, L. Tang, D. Klumpar, and R. Pfaff, Geophys. Res. Lett. **25**, 2053 (1998).
[54] R. S. Spangler, E. E. Scime, and G. Ganguli, Bull. Am. Phys. Soc. **46**, 167 (2001).
[55] J. Penano and G. Ganguli, Phys. Rev. Lett. **83**, 1343 (1999).
[56] J. R. Penano and G. Ganguli, J. Geophys. Res. **105**, 7441 (2000).
[57] S. R. Cranmer, Astrophys. J. **532**, 1197 (2000).